



Performance of Distance Protection in Presence of SVC Using Neural Network Approach

Mohammad A. Alziq¹, Eyad A. Feilat²

¹AES Jordan Power Plant Affiliation, Jordan

²The University of Jordan, Jordan, e.feilat@ju.edu.jo

Received Date: November 28, 2025 Accepted Date: December 31, 2025 Published Date : January 07, 2026

ABSTRACT

Shunt static VAR compensation has become a desired and effective solution for improving power transfer capability, voltage regulation and system stability. SVC has a significant impact on the impedance of the line, which in turn affects the accuracy of the impedance measurement. Transmission lines equipped with conventional distance relays may mal-operate in the presence of VAR compensators which in turn affect the accuracy the measured apparent impedance seen by the distance relay during a fault from the relay location to the fault point. The accuracy of the distance measurement is affected by the amount of compensated reactive power injected or absorbed by the VAR compensator. In that sense, the distance relay may under-reach or over-reach depending on the amount of compensation. In this paper, an artificial neural network approach is proposed to enhance the zone classification of distance relay. The proposed method is tested on a 400kV transmission line using Matlab/Simulink software. Extensive simulations are performed for various faults and over wide range of VAR compensation levels, fault locations, and fault types. These data sets are processed as neural network training/testing data. The simulation results showed high accuracy and speed of zone classification within less than three cycles.

Key words: Protection, distance relay, SVC, VAR compensation, neural network, FACTS, simulation.

1. INTRODUCTION

Flexible AC transmission system (FACTS) devices have become desired and effective solutions for improving power transfer capability and power system stability of long transmission lines [1-4]. A detailed modeling of distance relay and STATCOM was presented using PSCAD/EMTDC software [5-7]. Mal-operation of the distance relay, in the presence of Static Synchronous Series Compensator (SSSC), was presented in [8, 9]. An adaptive distance relay setting for the first zone in the presence of SSSC using artificial neural network (ANN) was presented [10]. The ANN was used to predict the new impedance settings of the distance relay.

A Static VAR Compensator (SVC) is one of the shunt FACTS devices that can be connected at the middle point of a transmission line to enhance voltage regulation on the line by controlling the injected or absorbed reactive power. In an SVC, the reactive power is absorbed through thyristor controlled reactor (TCR) and injected through thyristor switched capacitor (TSC). The apparent impedance and trip boundaries seen by conventional distance relay in the presence of an SVC at the middle of a transmission line was investigated [11-14]. Adaptive distance protection schemes for transmission lines incorporating (SVC) were presented [15-17].

In this paper, an ANN based approach is proposed to enhance the zone classification of the distance relay. The proposed method utilizes the SVC operational parameters and the measured impedance as input data to the neural network. The proposed method is tested on a 400kV transmission system using Matlab/Simulink software. Extensive simulations are performed for various faults and over wide range of VAR compensation levels, fault location, and fault type. These data sets are processed as neural network training data.

2. DISTANCE PROTECTION

Use either SI (MKS) or CGS as primary units. (SI units are strongly encouraged.) English units may be used as secondary

2.1 Principle of Distance Relay

Distance relays are widely used in protection systems to protect transmission lines because of their simplicity and reliability. A distance relay is able to detect a fault in a transmission line based on measuring the impedance of the transmission line, which is a function of the line length. Generally, the reach point in a distance relay is determined by the impedance per kilometer and the fault location on the transmission line. Nowadays, digital distance relays have widely replaced electromechanical and static distance relays. A distance relay measures the apparent impedance using current and voltage signals on the basis of Ohm's Law ($Z=V/I$) and compares this measured value with pre-set values. If the impedance is below the set value, this means that internal fault

has occurred. Accordingly, the relay immediately sends a trip signal to the circuit breakers to clear the fault. Otherwise, if the measured impedance is higher than the set value, this implies that the fault is external [18]. The impedance seen by the distance relay is calculated from secondary quantities of voltage and current as in (1). These values are affected by the type of fault, either line-to-line fault or line-to-ground fault. Therefore, during line-to-ground faults, a residual compensation factor k_0 is added to compensate for the zero-sequence impedance. This factor depends on the impedance parameters of the transmission line as stated in (2).

$$Z_{app} = \frac{V_R}{I_R} \quad (1)$$

$$k_0 = \frac{Z_0 - Z_1}{Z_1} \quad (2)$$

where V_R and I_R are the secondary values of the voltage and current signals, Z_0 and Z_1 are the transmission line zero and positive sequence impedances, respectively. Table 1 presents the relay measured voltage and current values for different types of faults, where A, B and C indicates system three phases, and G indicates the Ground.

Table 1: Voltage and current combinations used for detecting LG, LL and LLL faults

| Fault Type | V_R | I_R |
|------------|-------|-------------------------|
| LG | AG | $I_a + k_0 I_0$ |
| | BG | $I_b + k_0 I_0$ |
| | CG | $I_c + k_0 I_0$ |
| LL | AB | $I_a - I_b$ |
| | AC | $I_a - I_c$ |
| | BC | $I_b - I_c$ |
| LLL | ABC | I_a or I_b or I_c |

Normally, distance relay provides three stepped protection zones for transmission lines as main and backup protection. Figure 1 shows the three protection zones and the corresponding operating time-distance diagram. Zone 1 protects 80%-90% of the intended line instantaneously. Zone 2 provides backup protection for the remaining 10%-20% of the line which is not covered by zone 1, usually set to overreach the line from 120% to 150% but not beyond zone 1 of the adjacent line with operating time delay of 300 ms to achieve coordination with zone 1. Finally, zone 3 is set from 120% to 180% of the adjacent line with operating time delay of 600 ms to achieve coordination with zone 2.

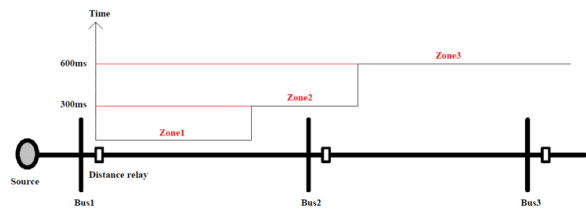


Figure 1: Distance Protection Zone and Time-Distance Diagram

2.2 Effect of Infeed on Measured Impedance

In distance protection, one of the main factors affecting the performance of the distance relay is the infeed current. When two or more power sources are connected to a protected line by a distance relay, the effect of the infeed current must be addressed since the fault current is fed from more than one direction, as depicted in Figure 2. The impedance seen by the distance relay for a fault is greater than the actual apparent impedance of the fault.

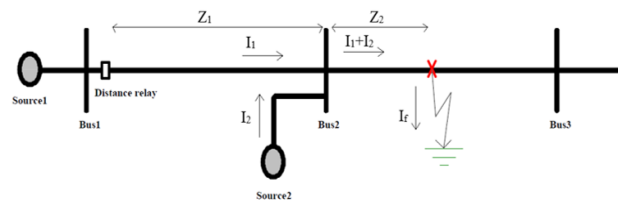


Figure 2: Effect of Infeed on Measured Impedance

For a solid fault, the voltage at bus1 at the relay location is given as in (3)

$$V_1 = I_1 Z_1 + (I_1 + I_2) Z_2 \quad (3)$$

The apparent impedance seen by the distance relay at bus1 is calculated as in (4)

$$\frac{V_1}{I_1} = Z_1 + \left(1 + \frac{I_2}{I_1}\right) Z_2 \quad (4)$$

$$Z_{seen} = Z_1 + (1 + K) Z_2 \quad (5)$$

where $K = I_2/I_1$ is the infeed factor.

Equation (5) indicates the inaccuracy induced by the infeed current in the measured impedance. Depending on the value of the infeed current, this inaccuracy might significantly influence the impedance, causing the distance relay to under-reach as the impedance seen by the distance protection relay is greater than the apparent impedance of the fault. The relay sees the fault farther than the actual fault location. On the other hand, the relay over-reaches when the impedance seen by the distance relay is less than the apparent impedance of the fault. In other words, it sees the fault closer than the actual fault location. As a result, this current contribution must be considered while establishing the zone settings of the distance relay.

3. STATIC VAR COMPENSATOR (SVC)

3.1 Construction of SVC

The SVC is one of the shunt FACTS devices that can be connected to a transmission line to increase the power transfer capabilities as well as to enhance the power quality through voltage regulation and support to prevent voltage instability, improving the power factor, reducing harmonics, and damping of power oscillation [4]. The SVC is an automatic impedance matching device that responds almost instantaneously to changes in the system voltage and provides VAR compensation, which gives it a significant advantage over basic mechanically switched compensation devices. A simplified scheme of an SVC is shown in Figure 3 [19]. Basically, the SVC is comprised of the following components:

1. Continuous thyristor-controlled reactor (TCR).
2. On/off thyristor switched capacitor (TSC).
3. A low-order harmonic filters for mitigating harmonics produced by the TCR.
4. Controller to control the absorbed or injected reactive power by changing the SVC from inductive to capacitive mode.

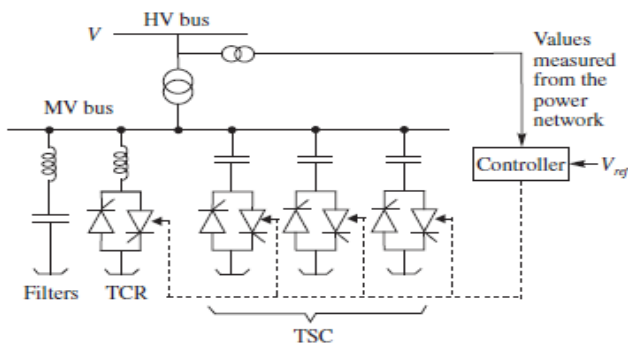


Figure 3: Typical Static Var Compensator (SVC)

3.2 Impact of SVC on Relay Performance

The impact of an SVC connected at mid-point of a transmission line on the measured impedance seen by a distance relay that is installed between bus 1 and bus 2 as shown in Figure 4 is analyzed.

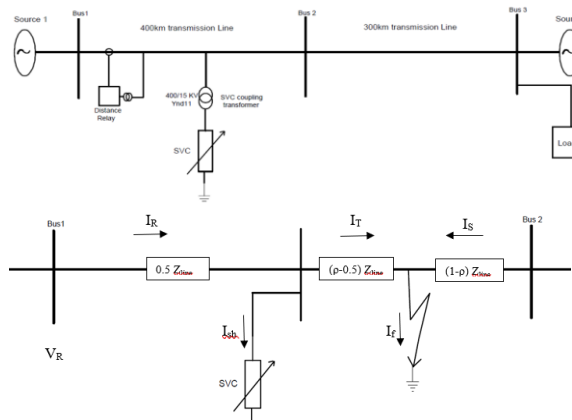


Figure 4: One-Line Diagram with Mid-Point Connected SVC

For a fault beyond the mid-point of the line the positive, negative and zero sequence components of the voltages and currents measured by the relay are expressed in (6)-(11).

$$I_{T1} = I_{R1} + I_{sh1} \quad (6)$$

$$I_{T2} = I_{R2} + I_{sh2} \quad (7)$$

$$I_{T0} = I_{R0} + I_{sh0} \quad (8)$$

$$V_{R1} = 0.5I_{R1}Z_{line1} + I_{T1}(\rho - 0.5)Z_{line1} \quad (9)$$

$$V_{R2} = 0.5I_{R2}Z_{line2} + I_{T2}(\rho - 0.5)Z_{line2} \quad (10)$$

$$V_{R0} = 0.5I_{R0}Z_{line0} + I_{T0}(\rho - 0.5)Z_{line0} \quad (11)$$

where V_{R1} , V_{R2} , V_{R0} , I_{R1} , I_{R2} , and I_{R0} are the positive, negative and zero sequence components of voltage and current at the relay bus respectively. Z_{line1} , Z_{line2} , and Z_{line0} are the positive, negative and zero sequence components of the transmission line. I_{sh1} , I_{sh2} , and I_{sh0} are positive, negative and zero sequence impedances of shunt injected current by the SVC. ρ is per unit distance of fault from relaying bus. The phase-A voltage at the relaying bus is V_{Ra} which can be obtained from the sequence components as given in (12):

$$V_{Ra} = V_{R1} + V_{R2} + V_{R0} \quad (12)$$

$$V_{Ra} = \rho I_{Ra}Z_{line1} + [(\rho - 0.5)(Z_{line0} - Z_{line1})I_{sh1} + I_{sh0}] + \rho I_{R0}(Z_{line0} - Z_{line1}) \quad (13)$$

Considering the SVC connected to the system through ΔY connected coupling transformer, the zero-sequence current of the SVC I_{sh0} can be eliminated. Accordingly, Equation (13) becomes

$$V_{Ra} = \rho I_{Ra}Z_{line1} + [(\rho - 0.5)(Z_{line0} - Z_{line1})I_{sh1} + \rho I_{R0}(Z_{line0} - Z_{line1})] \quad (14)$$

Following some mathematical manipulations, the apparent impedance seen by the relay for a LG is given as in (15), and for a LL or a LLL fault, the app impedance is calculated as in (16).

$$Z_{app} = \rho Z_{line1} + \frac{I_{sh1}}{I_{Rn} + k_n I_{R0}} (\rho - 0.5)Z_{line1} \quad (15)$$

$$Z_{app} = \rho Z_{line1} + \frac{I_{sh}}{I_R} (\rho - 0.5)Z_{line1} \quad (16)$$

4. SIMULATION RESULTS

4.1 System Under Study

The impact of the SVC on the distance relay is investigated through Matlab/Simulink simulation for different fault locations, fault types, and over wide range of operational modes of the SVC. Figure 5 depicts the three-line diagram model of a 50 Hz, 400kV transmission line connecting two AC systems with a SVC connected at the middle of the line. The transmission line parameters are given in Table 2

4.2 Size of the SVC

The SVC that is used in the study system consists of one 185 MVAR TCR bank and three 70 MVAR TSC banks that are connected at mid-point of the line via a 400 kV/15 kV (Yg/d11), 330 MVA coupling transformer, shown in Figure 6. Each three-phase bank is Y-connected. The secondary reactive power can be discretely varied from zero to 210 MVAR capacitive in steps of 70 MVAR by switching the TSCs on and off, while phase control of the TCR allows a liner variation from zero to 185 MVAR inductive.

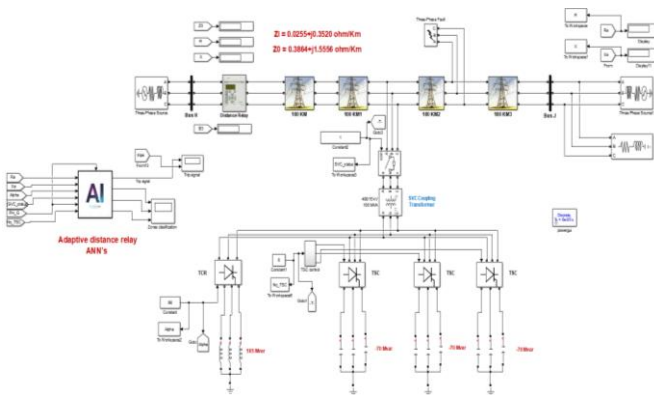


Figure 5: Three-Phase Simulink Model of the System under Study

Table 2: Transmission Line Parameters

| Parameter | Impedance |
|-------------------------------------|------------------------------|
| Positive sequence resistance R_1 | 25.5 m Ω /km |
| Zero sequence resistance R_0 | 386.4 m Ω /km |
| Positive sequence inductance L_1 | 1.12×10^{-3} H/km |
| Zero sequence inductance L_0 | 4.9516×10^{-3} H/km |
| Positive sequence capacitance C_1 | 12.74×10^{-12} F/km |
| Zero sequence capacitance C_0 | 7.75×10^{-12} F/km |

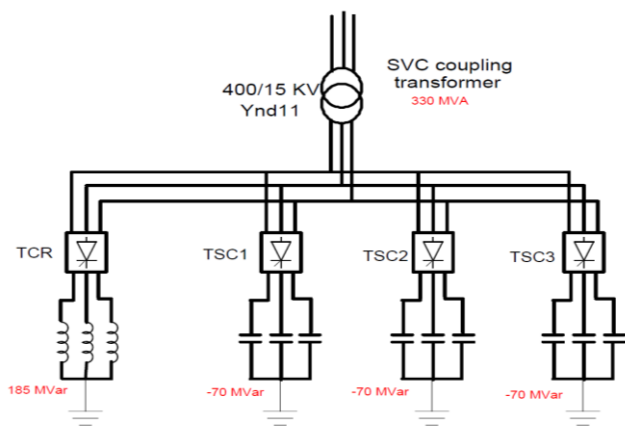


Figure 6: Three-Phase SVC Scheme with TCR and TSC

4.3 Settings of the Distance Relay

A three-step distance relay with Mho characteristics is implemented in this work. The setting of the three zones are as follows:

- Line impedance: $Z_{line} = 41.169 \angle 85.9^\circ \Omega$
- Zone 1 setting: 80% of the protected line with instantaneous response, $Z_{1set} = 112.93 \angle 85.9^\circ \Omega$
- Zone 2 is set to cover 125 % of the line with 300ms time delay, $Z_{2set} = 176.5 \angle 85.9^\circ \Omega$
- Zone 3 is set to cover 180 % of the line with 600ms time delay, $Z_{3set} = 254.1 \angle 85.9^\circ \Omega$

The distance relay is modeled in MATLAB and simulated using Simulink software.

4.4 Response of the Distance Relay

The impedance trajectories and the corresponding circuit breaker trip signals are demonstrated for several LG, LL and LLL faults at different locations along the line. This procedure is conducted for two cases, one case with the SVC disconnected and the other case with the SVC connected with two VAR levels of 200 MVAR (supplied) and -210 MVAR (absorbed). The fault inception is assumed occurring at $t = 0.5$ s.

4.4.1 Response of the Distance Relay to LG Fault

The impedance trajectories seen by the distance relay at bus 1 for a LG fault at 40% of line length of phase A (Zone 1) are shown in Figure 7. Several fault cases are investigated with and without SVC. It can be seen that the impedance trajectory eventually ends at the fault location in Zone 1, and the measured impedance is not affected by the presence of the SVC or VAR compensation level as the fault location is below the SVC location.

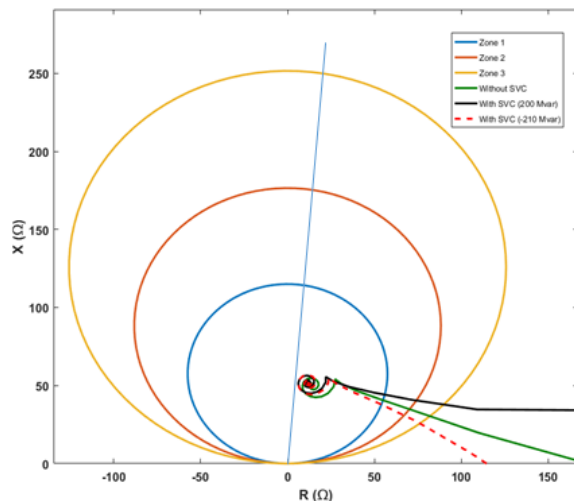


Figure 7: Impedance Trajectory for LG Fault at 40% of Line Length

The response of the trip signal and the fault current are depicted in Figure 8. Examining the response of the relay, one can see that the relay was able to detect accurately the fault and to issue the trip the signal immediately following the fault inception at $t = 0.52$ s.

The impedance trajectories seen by the relay and the corresponding fault current and trip signal for a LG fault at 75% of line length i.e. beyond the SVC location are illustrated in Figures 9 and 10, respectively. Figure 9 shows that when the SVC is disconnected, the trajectory of the measured impedance terminates in Zone 1. However, when the SVC is connected it can be seen that the relay under-reaches as the impedance trajectory ended at a point farther than the fault location in Zone 2, regardless the SVC is supplying or absorbing VARs, resulting in mal-tripping of the relay after time delay though the fault lies in Zone 1. Therefore, the relay did not trip instantaneously for a fault in zone 1. Instead, Zone 2 detected the fault and tripped the breaker after a time delay of 0.3s, as illustrated by the trip signal and fault current response shown in Figure 10.

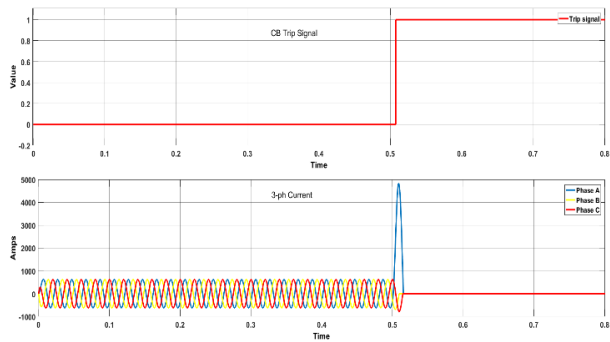


Figure 8: Relay Response for LG Fault in Zone 1

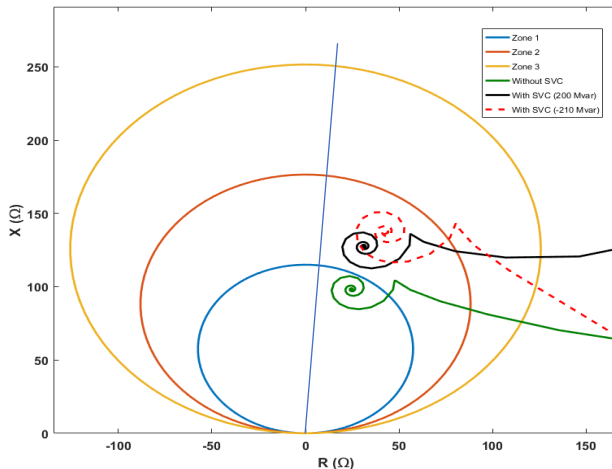


Figure 9: Impedance Trajectory for LG Fault at 75% of Line Length

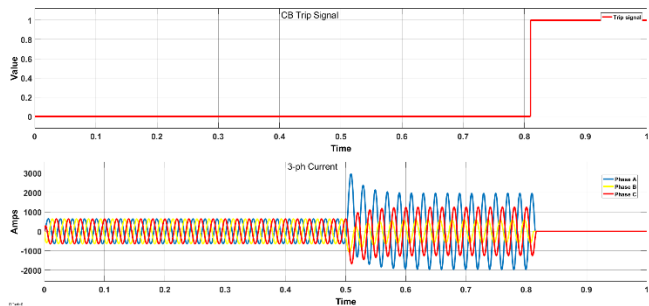


Figure 10: Relay Response for LG Fault in Zone 1

4.4.2 Response of the Distance Relay to LLG Fault

The impedance trajectories for a LL fault at 70% of line length are shown in Figure 11. It can be observed that the impedance trajectory ends at fault location in Zone 1, and it can be noticed that the measured impedance is not affected by the presence of the SVC or the compensation level.

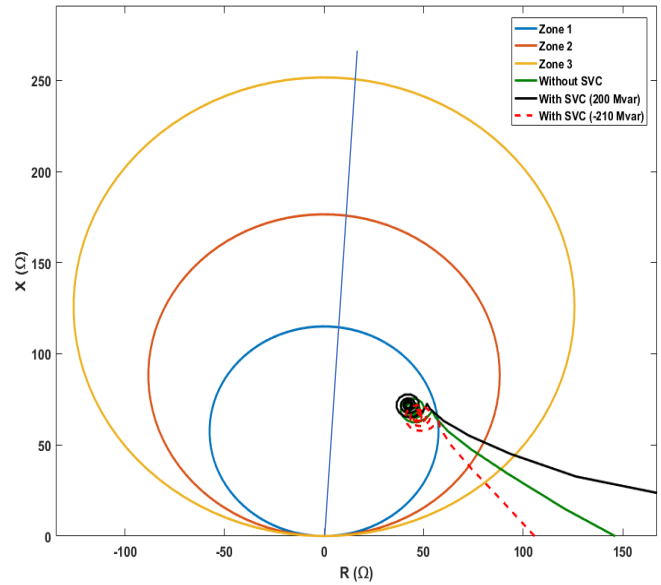


Figure 11: Impedance Trajectory for LL Fault at 70% of Line Length

4.4.3 Response of the Distance Relay to LLL Fault

Likewise, the impedance trajectories for a LLL fault at 70% of line length are depicted in Figure 12. Regardless the presence of the SVC or compensation level, one can see that the trajectories end exactly at fault location on the line in Zone 1.

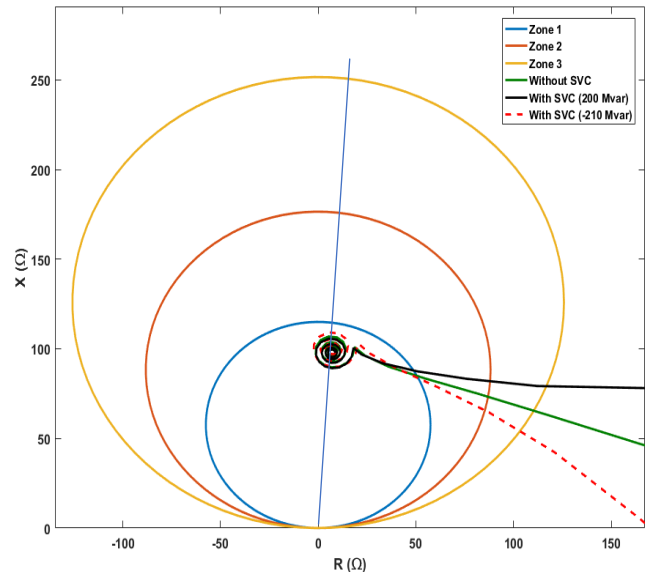


Figure 12: Impedance Trajectory for LLL Fault at 70% of Line Length

5. ANN BASED RELAY

To overcome the problem of under-reach of the conventional distance relay, in particular for a LG fault, an ANN-based relay is proposed. A back-propagation feedforward neural network is developed. The ANN comprises three layers; an input layer of 6 inputs, a hidden layer of 10 neurons with sigmoid activation functions, and an output layer of 3 outputs with softmax function. The 6 inputs of the network include the real and imaginary parts of the measured apparent impedance and the SVC operational parameters. The architecture of the proposed ANN ($6 \times 10 \times 3$) is shown in Figure 13. The outputs of the ANN represent the classification of three zones, as indicated in Table 3.

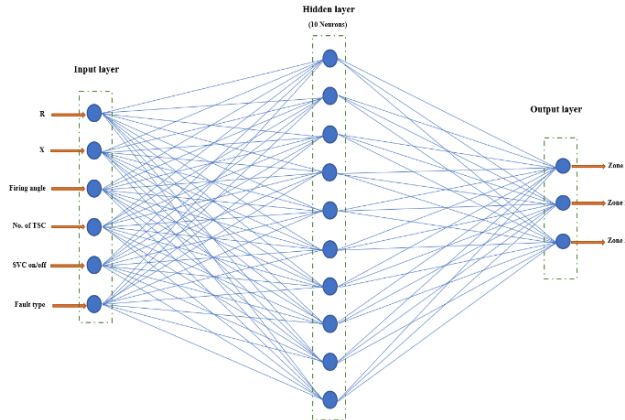


Figure 13: Architecture of the Neural Network Zone Classification

Table 3: ANN Output Classification

| Class | Output |
|--------|--------|
| Zone 1 | 1 0 0 |
| Zone 2 | 0 1 0 |
| Zone 3 | 0 0 1 |

To train the ANN and generalize its classification capability, a total of 9504 fault cases have been simulated on the system under study with various parameter combinations that cover all operation modes of the SVC and different fault locations, as presented in Table 4. The data is divided into 70% training data, 15% validation data, and 15% testing data.

The zone classification ANN was trained using the scaled conjugate gradient backpropagation training function (trainscg). It was chosen as it is faster as compared to other alternative training functions [20]. Figure 14 shows the training, validation, and testing mean square error (MSE) convergence curves. Figure 15 depicts the all confusion matrix related to training, validation, and testing phases. A precision of 99.20% is achieved.

The proposed ANN-based zone classification distance relay has been simulated using MATLAB/Simulink for a LG fault at

70% of line length with full inductive operation mode of the SVC. Figure 16 shows the ANN's output zone classification. Correct operation and zone classification of the proposed relay is obtained.

Table 4: Different Parameters of Fault Cases which are used to Generate Training Data for the ANN

| Fault Location (km) | TCR firing angle (α°) | Fault Type | Number of TSC | SVC Status |
|---------------------|-------------------------------------|------------|---------------|------------|
| 50 | 90 | AG | 0 | On |
| 80 | 100 | AB | 1 | Off |
| 100 | 110 | AC | 2 | - |
| 150 | 120 | ABG | 3 | - |
| 180 | 140 | ACG | - | - |
| 210 | 130 | ABC | - | - |
| 240 | 150 | - | - | - |
| 270 | 160 | - | - | - |
| 300 | 170 | - | - | - |
| 320 | - | - | - | - |
| 350 | - | - | - | - |
| 380 | - | - | - | - |
| 400 | - | - | - | - |
| 450 | - | - | - | - |
| 500 | - | - | - | - |
| 550 | - | - | - | - |
| 600 | - | - | - | - |
| 650 | - | - | - | - |
| 700 | - | - | - | - |
| 800 | - | - | - | - |
| 850 | - | - | - | - |
| 900 | - | - | - | - |

The zone classification ANN was trained using the scaled conjugate gradient backpropagation training function (trainscg). It was chosen as it is faster as compared to other alternative training functions [20]. Figure 14 shows the training, validation, and testing mean square error (MSE) convergence curves. Figure 15 depicts the all confusion matrix related to training, validation, and testing phases. A precision of 99.20% is achieved.

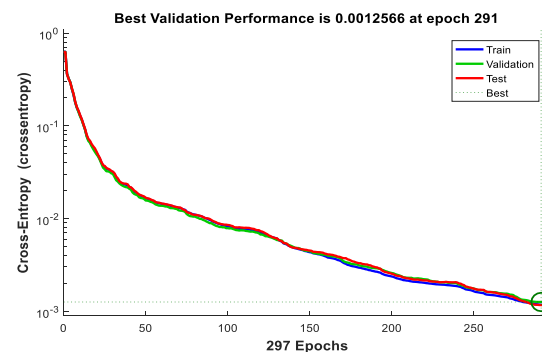


Figure 14: Training, Validation, and Testing Convergences Curves

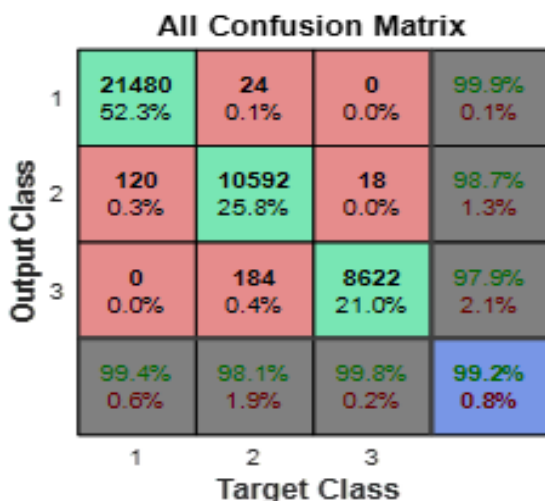


Figure 15: All Confusion Matrix

The proposed ANN-based zone classification distance relay has been simulated using MATLAB/Simulink for a LG fault at 70% of line length with full inductive operation mode of the SVC. Figure 16 shows the ANN's output zone classification. Correct operation and zone classification of the proposed relay is obtained.

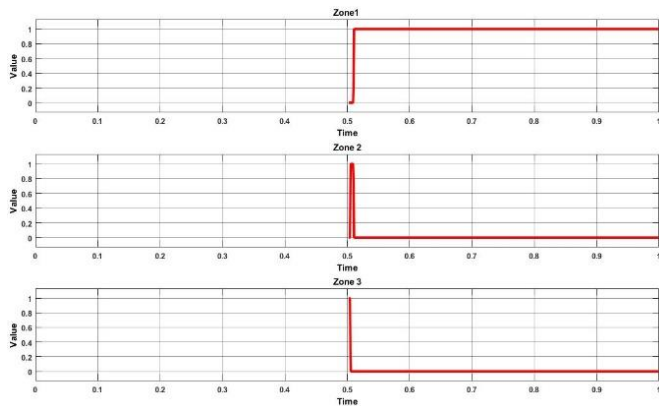


Figure 16: ANN Zone Classification for LG Fault at 70% of Line Length

CONCLUSION

In this paper, the effect of a SVC connected at mid-point of a transmission line protected using conventional distance relay has been investigated. The performance of the relay was tested for several types of fault and at different locations. It was found that the relay suffers under-reach problem in particular for LG fault beyond the SVC location. To improve the relay performance, an ANN has been developed to classify the fault location in the particular zone. The simulation results showed that ANN-based fault detection and zone classification achieved an accuracy of 99.2%. The proposed technique is effective and can be recommended to improve the performance of a conventional distance relay for VAR

compensated transmission lines.

ACKNOWLEDGEMENT

The authors would like to acknowledge the support and facilities provided by The University of Jordan.

REFERENCES

1. M.Eremia, C-C Liu, A-A. Edris, *Advanced solutions in power systems: HVDC, FACTS, and Artificial Intelligence*, Wiley-IEEE Press, 2016..
2. S. Chen, B. Mulgrew, and P. M. Grant. A clustering K.K. Sen, M.L. Sen, *Introduction to FACTS Controllers: Theory, Modeling and Applications*, John Wiley & Sons, Inc., and IEEE, New Jersey, USA, July 2009.
3. P.K. Dash, A.K. Pradhan, G. Panda, “**Apparent Impedance Calculations for Distance Protected Transmission Lines Employing Series-Connected FACTS Devices**,” *Electric Power Components and Systems*, Vol. 29, No. 7, July 2001, pp. 577-595.
4. P.K. Dash, A.K. Pradhan, G. Panda, A.C. Liew, “**Digital Protection Of Power Transmission Lines in The Presence Of Series Connected FACTS Devices**,” *Proceedings of IEEE/PES Summer Meeting*, Washington, USA, 19 July, 2000, pp. 1967-1972.
5. N.G. Hingorani, L. Gyugyi, *Understanding FACTS: concepts and technology of flexible AC transmission systems*, Wiley-IEEE Press, 2000
6. D. Hemasundar, M. Thakre, V.S. Kale, “**Impact of STATCOM on distance relay-Modeling and simulation using PSCAD/EMTDC**,” *2014 IEEE Students' Conference on Electrical, Electronics and Computer Scienem*, 01-02 March 2014, Bhopal, India.
7. T.S. Sidhu, R.K., Varma, P.K., Gangadharan, F. A., Albasri, G.R. Ortiz, “**Performance of distance relays on shunt-FACTS compensated transmission line**,” *IEEE Trans. on Power Delivery*, Vol. 20, No.3, July 2005, pp.1837-1845.
8. W-H. Zhang, S-J.Lee, M-S.Chi, S. Oda, “**Considerations on distance relay setting for transmission line with STATCOM**,” *IEEE PES General Meeting*, 25-29 July 2010, Minneapolis, MN, USA.
9. A. Kazemi, S. Jamali, H. Shateri, “**Distance relay mal-operation due to presence of SSSC on adjacent lines in inter phase faults**,” *2008 IEEE Region 5 Conference*, 17-20 April 2008, Kansas City, MO, USA.
10. M. Khederzadeh, A. Ghorbani, A. Saleminia, “**Impact of SSSC on the digital distance relaying**,” *2009 IEEE Power & Energy Society General Meeting*, 26-30 July 2009, Calgary, AB, Canada.
11. H. Rastegar, A.P. Khansaryan, “**A new method for adaptive distance relay setting in the presence of SSSC using neural networks**,” *2006 1st IEEE Conference on Industrial Electronics and Applications*, 24-26 May 2006, Singapore.

12. A.S. Alayande, S.O. Akinbode, I.K. Okakwu, A.O. Oyedeleji, “**Performance analysis of static var compensators for distance protection of Nigerian 132-kV sub-transmission network using Matlab/Simulink model**,” MANAS Journal of Engineering, Vol. 10, No. 1, 2022, pp. 1-16.
13. S.K. Mishra, “**A neuro-wavelet approach for the performance improvement in SVC integrated wind-fed transmission line**,” Ain Shams Engineering Journal, Vol. 10, No. 3, September 2019, pp. 599-611.
14. A. Ghorbani, M. Khederzadeh, B. Mozafari, “**Impact of SVC on the protection of transmission lines**,” International Journal of Electrical Power & Energy Systems, Vol. 42, No. 1, 2012, pp. 702-709.
15. M. Zellagui, A. Chaghi, “. **Impact of SVC devices on distance protection setting zones in 400 kV transmission line**,” UPB Scientific Bulletin, Series C: Electrical Engineering and Computer Science, Vol. 7, No. 2, 2013, pp. 249-262.
16. A.R. Singh, S.S. Dambhare, “**Adaptive distance protection of transmission line in presence of SVC**,” International Journal of Electrical Power & Energy Systems, Vol. 53, December 2013, pp. 78-84.
17. S.B. Kulkarni, R.H. Chile, A.R. Singh, “**A Novel Fast Adaptive Digital Distance Protection of Transmission Line in Presence of SVC**,” Elektrika, July 2012, Vol. 14, No. 1, 2012, pp. 14-20.
18. M.P. Thakre, V.S. Kale, “An adaptive approach for three zone operation of digital **distance relay with Static Var Compensator using PMU**,” International Journal of Electrical Power & Energy Systems, Vol. 77, pp. 327-336.
19. S.H. Horowitz, A.G. Phadke, **Power System Relaying**, 4th Ed., John Wiley & Sons, 2014.